NACA TN 2681 9051

TECH LIBRARY KAFB, NM
0065655

NATIONAL ADVISORY COMMITTEE FOR AERONAUTICS

TECHNICAL NOTE 2681

A COMPRESSIBLE-FLOW PLOTTING DEVICE AND ITS APPLICATION TO CASCADE FLOWS

By Willard R. Westphal and James C. Dunavant

Langley Aeronautical Laboratory
Langley Field, Va.

Washington
April 1952

AFMDC
TECHNICAL LIBRARY
AFL 2811

TECH LIBRARY KAFB, NM

0065655

1A

NATIONAL ADVISORY COMMITTEE FOR AERONAUTICS

TECHNICAL NOTE 2681

A COMPRESSIBLE-FLOW PLOTTING DEVICE AND ITS APPLICATION TO CASCADE FLOWS

By Willard R. Westphal and James C. Dunavant

SUMMARY

A simplified method has been devised for the solution of two-dimensional compressible flows through well-defined passages. This method makes use of plastic cams which automatically set the length-to-width ratio of rectangles formed by streamlines and equipotential lines represented by spring-steel wires. Pressure distributions around four cascades of turbine blades and along the surface of a choked nozzle determined by this method are shown to compare well with experimental results.

INTRODUCTION

Two-dimensional flow problems may be solved by the potential-flow plotting method. Reference 1 describes a method of determining the velocity distribution for a cascade of turbine blades for incompressible, inviscid flow by the use of a wire-mesh flow plotting device. Since the local velocities on gas-turbine blades commonly reach sonic velocity, the effects of compressibility should be taken into account when solving for the blade-surface velocity distribution. The problem of plotting compressible flow is more difficult than that of plotting incompressible flow since the density is not constant but varies with velocity. For that reason, the rectangles formed by streamlines and equipotential lines of a flow plot are not curvilinear squares as in the incompressible case but vary in length-to-width ratio as the velocity varies in the field. In previous attempts to plot compressible flows, the length-to-width ratio of the rectangles has been adjusted individually. Brenner and Kilgore, in reference 2, attempted a solution by manually measuring the width and setting the length of each rectangle. Sells, of General Electric (reference 3), devised four-prong calipers which set the correct length when adjusted to width. In these methods the streamlines were adjusted individually in a time-consuming iterative process.

This paper describes a cam device which continuously maintains the correct length-to-width ratio of each rectangle formed by the streamlines

and equipotential lines which in this case are represented by spring-steel wires. The compressible, potential flow through well-defined passages such as high-solidity cascades, nozzles, and ducting can be obtained directly with this device. Comparisons of surface pressure distributions obtained with this device with high-speed cascade data are shown for four turbine-blade cascades. A two-dimensional nozzle shape redesigned with this device in order to avoid supersonic velocities along the surface of the nozzle was also studied.

SYMBOLS

a	speed of sound
C	constant
M	Mach number (V/a)
p	static pressure
q	dynamic pressure $\left(\frac{1}{2}\rho V^2\right)$
V	velocity
x	distance parallel to flow direction
y	distance normal to flow direction
ΔX	distance between equipotential lines
ΔY	distance between streamlines
β	inlet flow angle, angle between upstream velocity and normal to stagger line
γ	ratio of specific heats
θ	turning angle, angle between entering velocity and exiting velocity
Φ	potential function
ρ	density

Subscripts:

1	upstream
2	downstream
o	stagnation
cr	critical value; that is, value when local Mach number is 1.0

PRINCIPLES OF COMPRESSIBLE-FLOW PLOTTING

Design and construction of device.- In order to satisfy the equations of compressible potential flow, the flow plot must satisfy boundary conditions, have the length-to-width ratio of all rectangles equal to the ratio of local density to stagnation density, and maintain orthogonality of all intersecting streamlines and equipotential lines.

The compressible-flow plotting device consisted of a grid of wires representing streamlines and equipotential lines, pins at the intersection of the wires, and plastic cams which restrain the pins so that the rectangles formed by the wires have the proper length-to-width ratio. Figure 1 shows the arrangement of the cams, pins, and wires in a small element of the compressible-flow plotting device.

The wires were spring-tempered stainless steel. A diameter of 0.041 inch was selected for the wires as a compromise between the flexibility needed to meet boundary conditions and the stiffness needed to keep the streamlines and equipotential lines smoothly faired. The pins were of $\frac{1}{8}$-inch-diameter brass rod, $1\frac{1}{2}$ inches in length. Two holes were drilled in each pin for the wires 1/8 inch and 1/4 inch from the base at right angles to each other.

The cams (fig. 2) were manufactured by injection molding of a phenolic-resin plastic. The thickness of the cams was 0.060 inch and the width of the cam slot for the pins was $0.125 \begin{smallmatrix} +0.002 \\ -0.001 \end{smallmatrix}$ inch. The coordinates were accurate to ±0.003 inch. The range of Mach number for the cams was from 0.3 to 1.0. The maximum width of streamtubes for which the cams were designed was 1.760 inches and the minimum width was 0.864 inch. Small pointed pins were strung along the boundary streamlines and were pressed into a soft-wood board to fix the boundary conditions.

The shape of the slots of these cams was so designed that the width ΔY is the proper function of length ΔX. Since $d\Phi = V\,dx$ and the change in potential between adjacent lines of equal potential is constant, then

$$V = \frac{C}{\Delta X} \tag{1}$$

where C is an arbitrary constant chosen to give a convenient cam size. As already noted,

$$\frac{\Delta X}{\Delta Y} = \frac{\rho}{\rho_o} \tag{2}$$

For isentropic flow

$$\frac{\rho}{\rho_o} = \left[1 - \frac{\gamma - 1}{2}\left(\frac{V}{a_o}\right)^2\right]^{\frac{1}{\gamma-1}} \tag{3}$$

Substituting equations (1) and (3) into equation (2) and solving for ΔY gives

$$\Delta Y = \frac{\Delta X}{\left[1 - \frac{\gamma - 1}{2}\left(\frac{C}{\Delta X a_o}\right)^2\right]^{\frac{1}{\gamma-1}}} \tag{4}$$

The relation between ΔX and Mach number may be determined from the energy equation

$$\frac{1}{2}V^2 + \frac{1}{\gamma - 1}a^2 = \frac{1}{\gamma - 1}a_o^2$$

or, after the terms are rearranged,

$$\frac{V^2}{a^2} = M^2 = \frac{1}{\left(\frac{a_o}{V}\right)^2 - \frac{\gamma - 1}{2}} \tag{5}$$

By substituting equation (1) into equation (5), the Mach number in terms of ΔX is

$$M^2 = \frac{1}{\left(\frac{\Delta X\ a_o}{C}\right)^2 - \frac{\gamma - 1}{2}} \tag{6}$$

Equations (4) and (6) are plotted in figure 3 for a value of $C = \frac{a_o}{2}$ which gives a cam of convenient size if ΔX is measured in inches. As can be seen from this figure, the values of ΔX are difficult to determine accurately for values of ΔY near $M = 1.0$. The cam slots were designed from equation (4) for $\gamma = 1.40$. The coordinates measured from the cam center for each slot are $\Delta X/2$ and $\Delta Y/2$ (fig. 2); hence, the distance between identical points on the four slots is ΔX and ΔY. Each value of ΔX and ΔY on the cam corresponds to one Mach number which is given by equation (6). The cam slot was not designed to include supersonic velocities because the discontinuities present in supersonic flow cannot be treated.

Although it has not been shown mathematically, it was found experimentally that orthogonality was maintained by the cams alone with two exceptions, which are shown in figures 4(a) and 4(b). Although no wires were used with the pins and cams to obtain these patterns, lines connecting the intersections have been drawn in the figures to show the pattern of streamlines and equipotential lines. The first figure shows distortion which is equivalent to a displacement of the streamlines along a 45° line. In the second pattern (fig. 4(b)) the cams turned alternately and gave zigzag streamlines. Adding the wires prevents these extraneous patterns from occurring by smoothly fairing the streamlines and equipotential lines. The wires are also used to keep the pins vertical.

Since the cams are finite rather than infinitesimal in size, a difference exists between the distance measured along the curved streamline and the straight-line distance between pins. This difference depends on the radius of curvature and is insignificant for these cams for radii of curvature greater than 3 inches. Hence, any plot made must be of sufficient size so that a small radius of curvature is not present on any important boundary line and enough streamtubes are included to define the flow throughout the field.

Procedure.- The compressible-flow plotting device is constructed on a scale drawing of two passages of a cascade. One passage is sufficient if the boundary streamlines are made identical, but it is better to plot the flow in two or three passages to a point far enough past the nose to insure that the flow around the nose of the blades is correctly defined.

The scale of the drawing is uniquely determined by the scale of the cams, the number of streamtubes per passage, and the entering Mach number. In general, the scale of the drawing must be changed in order to vary the entering Mach number. The distance between two adjacent stagnation streamlines must be equal to the value of ΔY for the entering Mach number times the number of streamtubes between stagnation streamlines. Thus, by determining the distance between stagnation streamlines upstream, the scale of the drawing is found.

The complete grid of cams cannot be easily adjusted because of the great amount of friction on the cam surfaces. Hence, for each compressible-flow plot to be made, the grid of wires and pins should be shaped to the boundary conditions before adding the cams. The cams are added in rows starting from the uniform upstream flow. This procedure eliminates interference between cams since each cam is on a different level than the adjacent ones. Because of this procedure, the cams are slightly tipped both in the stream direction and normal to it (fig. 1). Measurements are made of the values of ΔX along the boundary lines and the Mach number is found for each measurement by equation (6). From a measured value of ΔX an average value of the velocity for a finite distance along the boundary can be found. This average velocity is considered to occur midway between the pins.

A check on the final result is that the normal-force coefficient computed from the integrated pressure distribution around the blade must correspond to the turning of the air through the cascade. Actually, the amount of turning through a given cascade is, to some extent, arbitrary; that is, in general, the inlet air angle, inlet Mach number, and cascade configuration are not sufficient to determine the exit air angle. Specifying the position of the trailing-edge stagnation point would make the problem unique. Assuming a local flow direction at the trailing-edge region is equivalent to assuming a position of the trailing-edge stagnation point. When the compressible-flow plotting device is used, the existence of boundary layer is recognized and the exiting flow is assumed to have no velocity peaks around the trailing edge; hence, the local streamlines leave with approximately the mean-line direction and with a wake thickness equal to or greater than the trailing-edge thickness. In the solutions that have been obtained with this device, this direction has been assumed as the exit direction for the first approximation, with some subsequent small adjustment of this direction, if necessary, in order to satisfy the criterion just mentioned. The adjustment is readily accomplished since it affects the turning angle directly but has almost no effect on the normal-force coefficient as computed from the pressures. For high-solidity cascades with relatively low entering velocities, the position of the nose stagnation point has only a small effect on the pressure distribution. For this reason, no attempt was made to determine the local velocities at the nose accurately.

COMPARISON WITH EXPERIMENTAL RESULTS

The device has been used to plot the flow through four turbine-blade cascades, and the pressure distributions measured from these plots are compared with those from high-speed cascade tests. Figure 5 shows the pressures obtained along the surface of an airfoil in an 88° turning cascade for an entering Mach number of approximately 0.34 for both the test and the flow plot. It can be noted from this figure that an irregularity of points occurs in the region of high velocity. This irregularity can be attributed to the large changes in ΔX (or velocity) that occur for small changes in ΔY at speeds approaching a Mach number of 1. A photograph of the plotting device for this cascade is shown as figure 6. Several cams were left out along the pressure surface of the blade because the Mach number in that region was below 0.3, which is the minimum value for which the cams were designed. In small low-speed areas such as this, the length-to-width ratio of the rectangles is adjusted manually rather than by using special large-size cams. The rectangles will become almost square as in an incompressible flow with a density ratio of 1.0 when the flow velocity is very low.

Figure 7 compares the pressure distributions obtained from a plot and from the cascade test for the same blade section as in figure 5 but at a higher inlet air angle. The difficulty of maintaining the boundary conditions around the highly curved nose and the high velocity in this region caused the difference in the pressure distributions.

Pressure distributions for a cascade similar to that shown in figure 5 are compared in figure 8. The same small amount of irregularity occurred in the pressure distribution obtained by the flow plotting device shown in this figure. There is no irregularity of points in the pressure distribution for the fourth cascade (fig. 9) which was a low-turning turbine cascade. Evidence in other plots also has shown that this irregularity of points occurred only in regions of high velocity and did not occur in a steep velocity gradient. Generally good agreement is shown between the pressure distributions of the cascade tests and the flow plots for the four cascades tested in spite of the approximations made at the nose.

The average length of time required to plot the flow through a turbine cascade is 8 hours, an appreciable reduction in time from that required with the incompressible-flow plotting device. The time reduction is due to the setting of the streamlines and equipotential lines by the cams. The accuracy of the plots made with the compressible-flow plotting device is generally good, results comparing equally as well as those of the incompressible-flow plotting device with cascade data. Reliability of the results should be much better for the cam device since the plot

required no alinement, positions of the streamlines being rigidly fixed by the cams.

All the plots were made for entering Mach numbers which were slightly below the critical value for the blade section so that the maximum Mach number along the blade surface would be less than 1.0 since the mechanical inaccuracies of the cams produce larger errors near sonic velocities. An effort has been made to determine the entering Mach number for which sonic velocity will first occur at some point along the blade surface. This Mach number is of value in comparing various blade sections.

A simple method which has been used to obtain the critical entering Mach number is to extrapolate the highest Mach number obtained on the blade surface in the flow plot to a Mach number of 1.0 by means of the Prandtl-Glauert extrapolation method (reference 4). To use this method, a mean passage Mach number is first calculated for the section of the passage where the maximum surface velocity occurred in the flow plot. This mean passage Mach number is best obtained from the upstream Mach number and the ratio of the area of flow upstream to the area of the passage at the point of maximum local Mach number. The mean passage Mach number is considered to be the equivalent of M_∞ in the Prandtl-Glauert extrapolation which is equation (8-41) of reference 4

$$C_p = \frac{C_{p_o}}{\sqrt{1 - M_\infty^2}}$$

where $C_p = \frac{p - p_\infty}{q_\infty}$ and C_{p_o} is the low-speed or incompressible value of the pressure coefficient. The extrapolation is made for a constant value of C_{p_o} from the condition of the flow plot to $\left(C_p\right)_{crit}$ which is given by equation (3-21) of reference 4

$$\left(C_p\right)_{crit} = \frac{2}{\gamma M_\infty^2}\left[\left(\frac{2}{\gamma + 1} + \frac{\gamma - 1}{\gamma + 1} M_\infty^2\right)^{\frac{\gamma}{\gamma-1}} - 1\right]$$

A single plot of these two equations facilitates their rapid simultaneous solution for the critical value of M_∞ or critical mean passage Mach number. The value of the mean passage Mach number at this critical point is then converted to a critical entering Mach number by using

the original area ratio. Critical entering Mach numbers computed by this method for the four flow plots and critical Mach numbers obtained in cascade tests are as follows:

	M_{cr}			
	First configuration	Second configuration	Third configuration	Fourth configuration
Cascade test	0.354	0.385	0.467	0.473
Compressible-flow plot	.356	.395	.524	.460
Maximum blade-surface Mach number	.838	.848	.867	.850

Very good agreement of the critical values is obtained except in the case where peak velocity obtained with the plotting device was in error (third configuration).

The compressible-flow plotting device was also used to determine the velocity distribution along the surface of a choked subsonic two-dimensional nozzle. The solution could not be made for the complete nozzle shape since the boundary streamline could not be made to conform to the nozzle surface where it was highly curved even though the local Mach number was 1.0. This deviation indicates that the velocity over the nozzle surface would have been supersonic. Hence, the boundary streamline along the surface was allowed to deviate slightly from the nozzle in the supersonic region to increase the radius of curvature so that supersonic velocities were avoided (fig. 10). Subsequent test of the nozzle shape confirmed the existence of a supersonic region along the surface of the nozzle where the compressible-flow plotting device indicated supersonic velocities. Surface Mach numbers along the unmodified section of the nozzle show reasonable agreement considering the fact that the velocities were very close to sonic and the compressible-flow plot was made without consideration of the boundary layer.

CONCLUDING REMARKS

The plotting device described herein simplifies the graphical solution of two-dimensional compressible-flow problems that would otherwise require long and tedious mathematical solutions. The cams used on the device greatly speed the solution by positioning the streamlines and equipotential

lines of the flow plot and compensating automatically and continuously for the change in density throughout the flow field.

Reasonable results were obtained for four turbine-blade cascades and a two-dimensional nozzle. Other configurations of the channel-flow type such as ducting, turning vanes, and passage shapes which are long compared to their width could be investigated by use of the compressible-flow plotting device.

Langley Aeronautical Laboratory
National Advisory Committee for Aeronautics
Langley Field, Va., January 15, 1952

REFERENCES

1. Westphal, Willard R., and Dunavant, James C.: Application of the Wire-Mesh Plotting Device to Incompressible Cascade Flows. NACA TN 2095, 1950.

2. Brenner, Wm. C., and Kilgore, Lee A.: Air Flow Determination by Graphical Methods. Preprint, Inst. Aero. Sci., Inc., 1944.

3. Poritsky, H., Sells, B., and Danforth, C. E.: Graphical, Mechanical and Electrical Aids for Compressible Fluid Flow. Data Folder 46150, Aircraft Gas Turbine Eng. Div., Gen. Elec. Co., Aug. 13, 1948.

4. Liepmann, Hans Wolfgang, and Puckett, Allen E.: Introduction to Aerodynamics of a Compressible Fluid. John Wiley & Sons, Inc., 1947, pp. 28, 244-245.

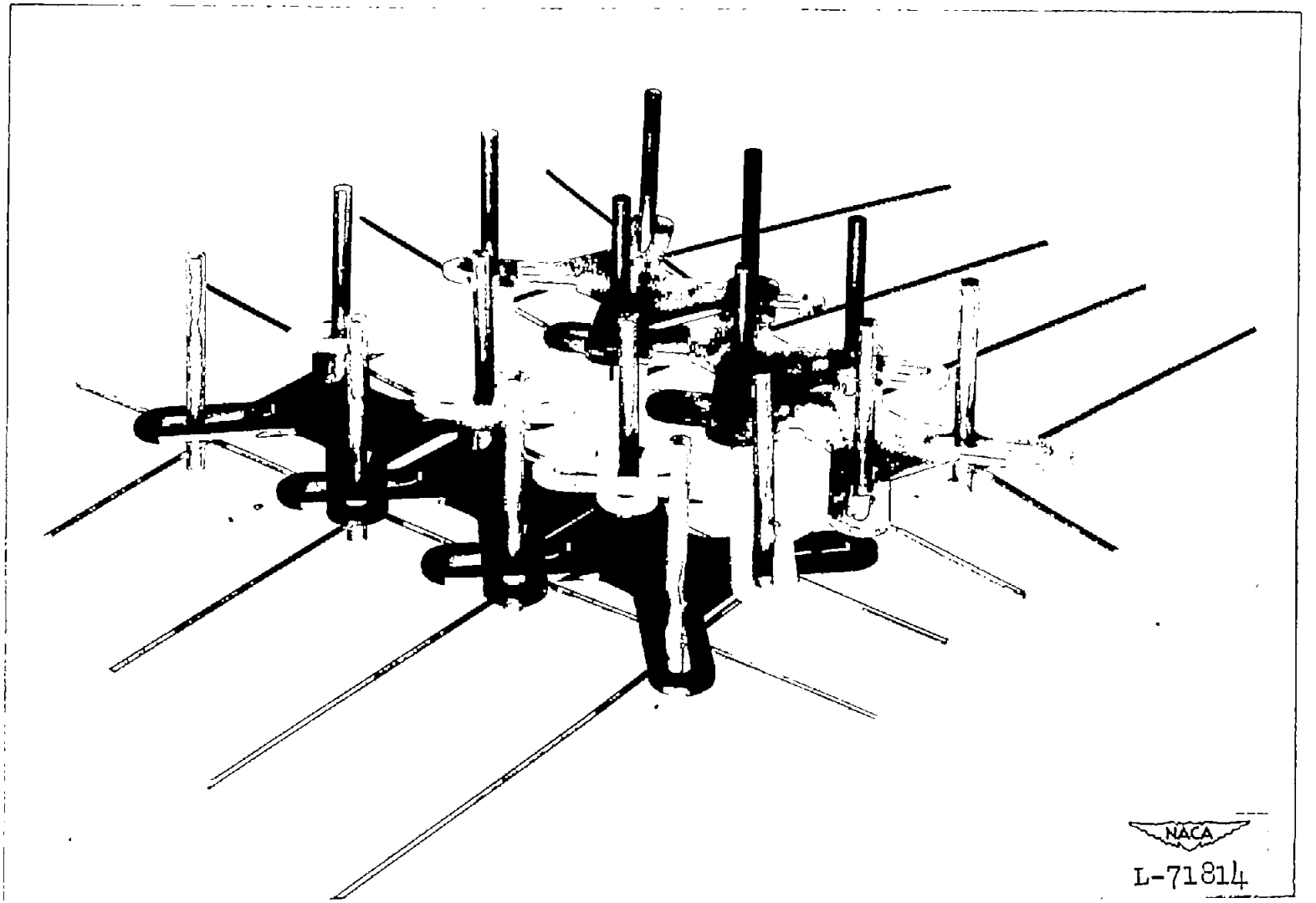

Figure 1.- A small element of the compressible-flow plotting device.

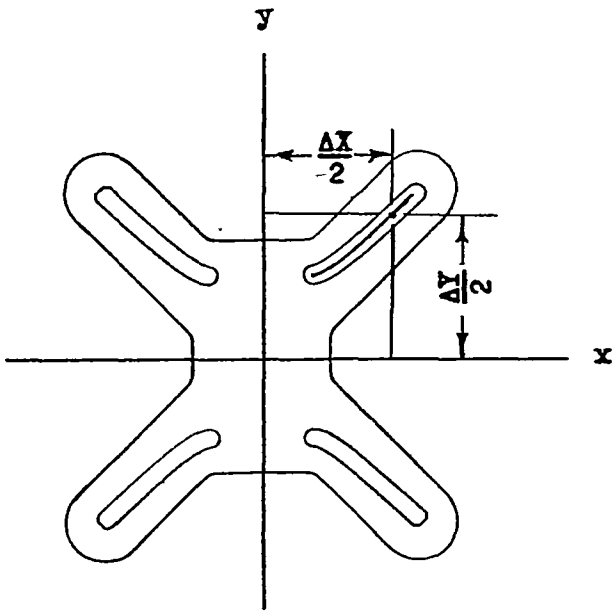

Cam ordinates	
$\frac{\Delta X}{2}$	$\frac{\Delta Y}{2}$
0.2740	0.4318
.2750	.4322
.3000	.4360
.3250	.4435
.3500	.4580
.3750	.4730
.4000	.4905
.4250	.5083
.4500	.5370
.5000	.5683
.5500	.6108
.6000	.6555
.6500	.7008
.7000	.7465
.7500	.7932
.8000	.8408
.8405	.8795

Figure 2.- Plastic cam and ordinates.

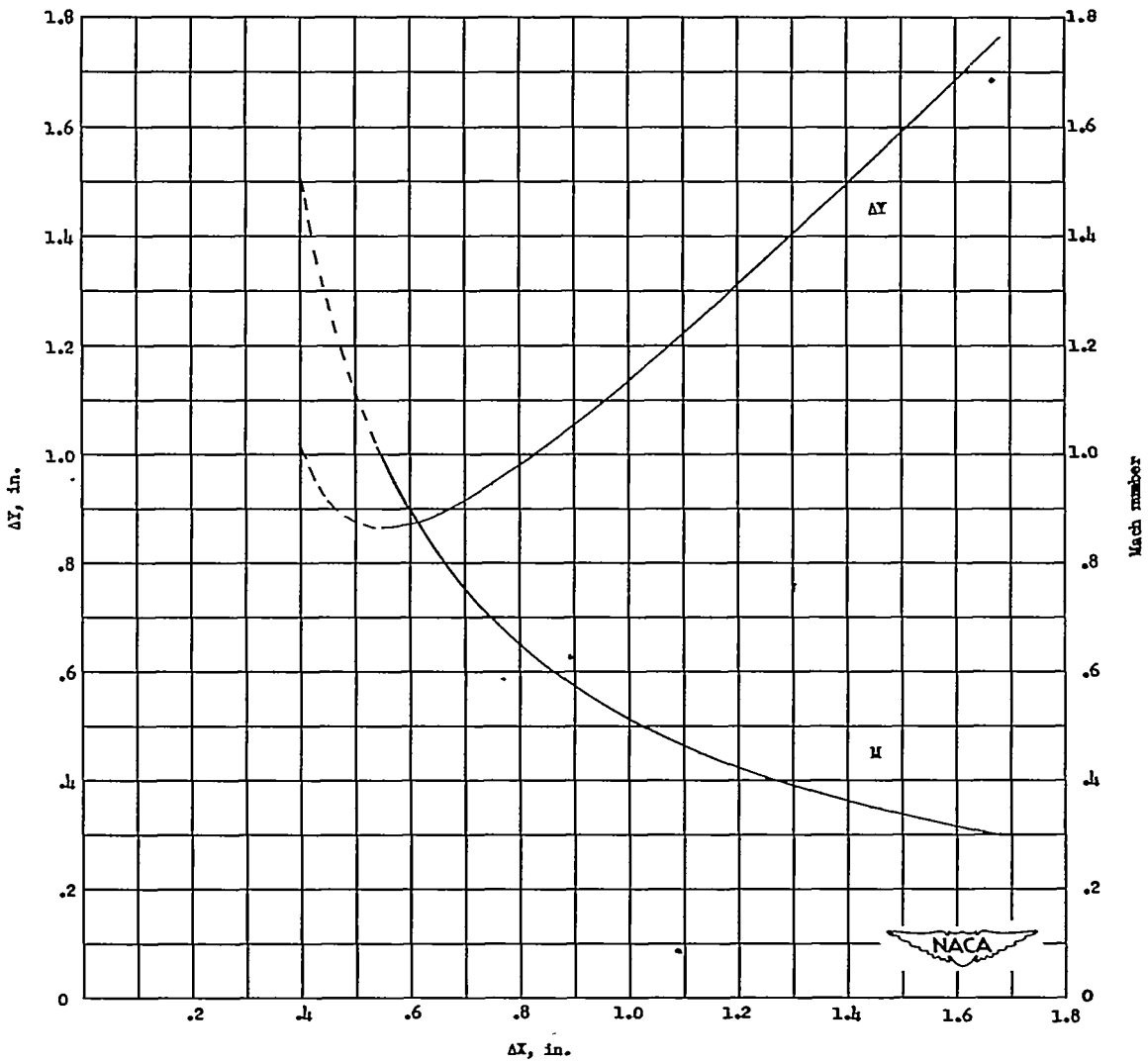

Figure 3.- Mach number for distances on cam. $\frac{C}{a_o} = \frac{1}{2}$.

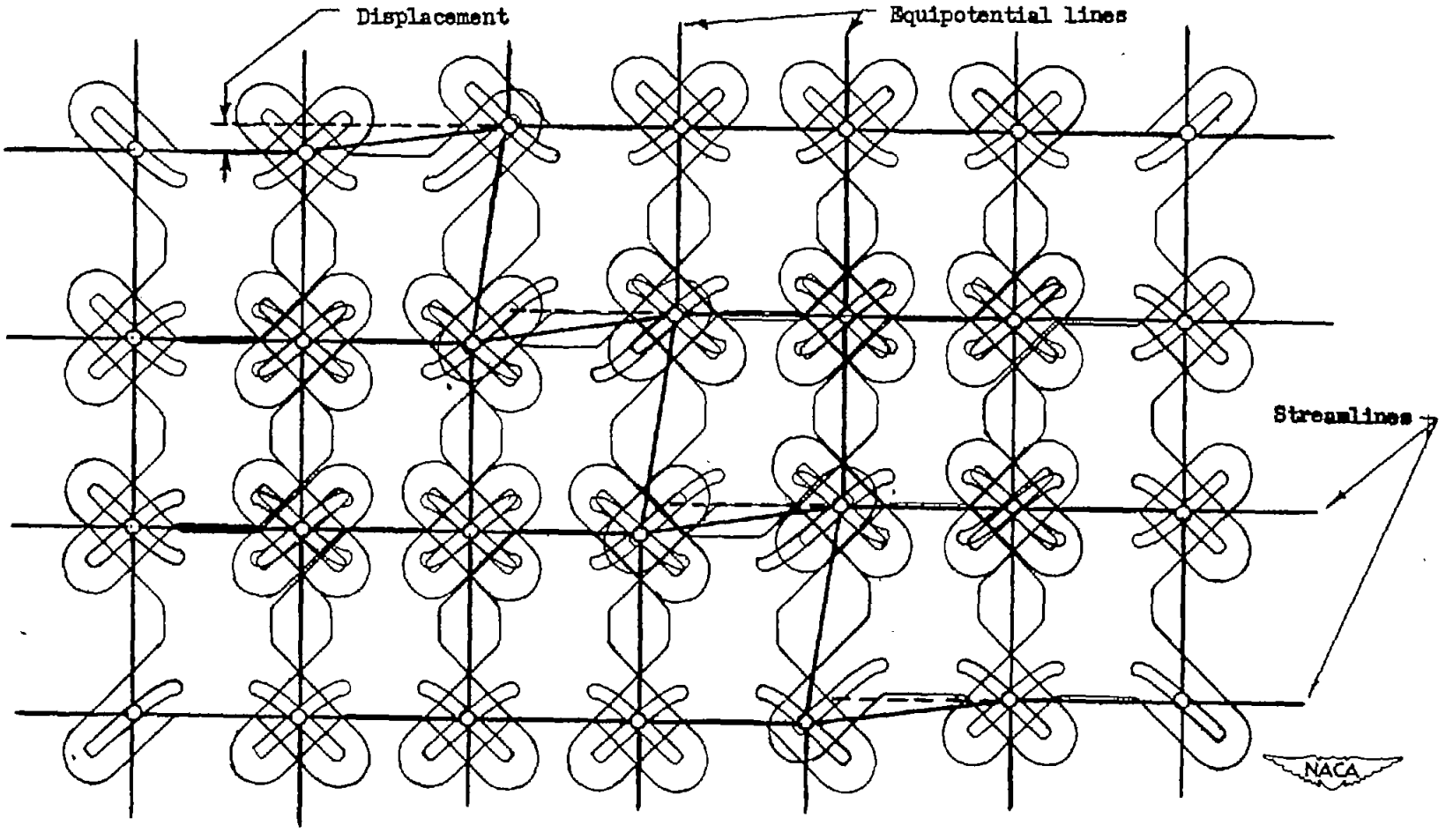

(a) Displacement along 45° line.

Figure 4.- Exceptions to orthogonality.

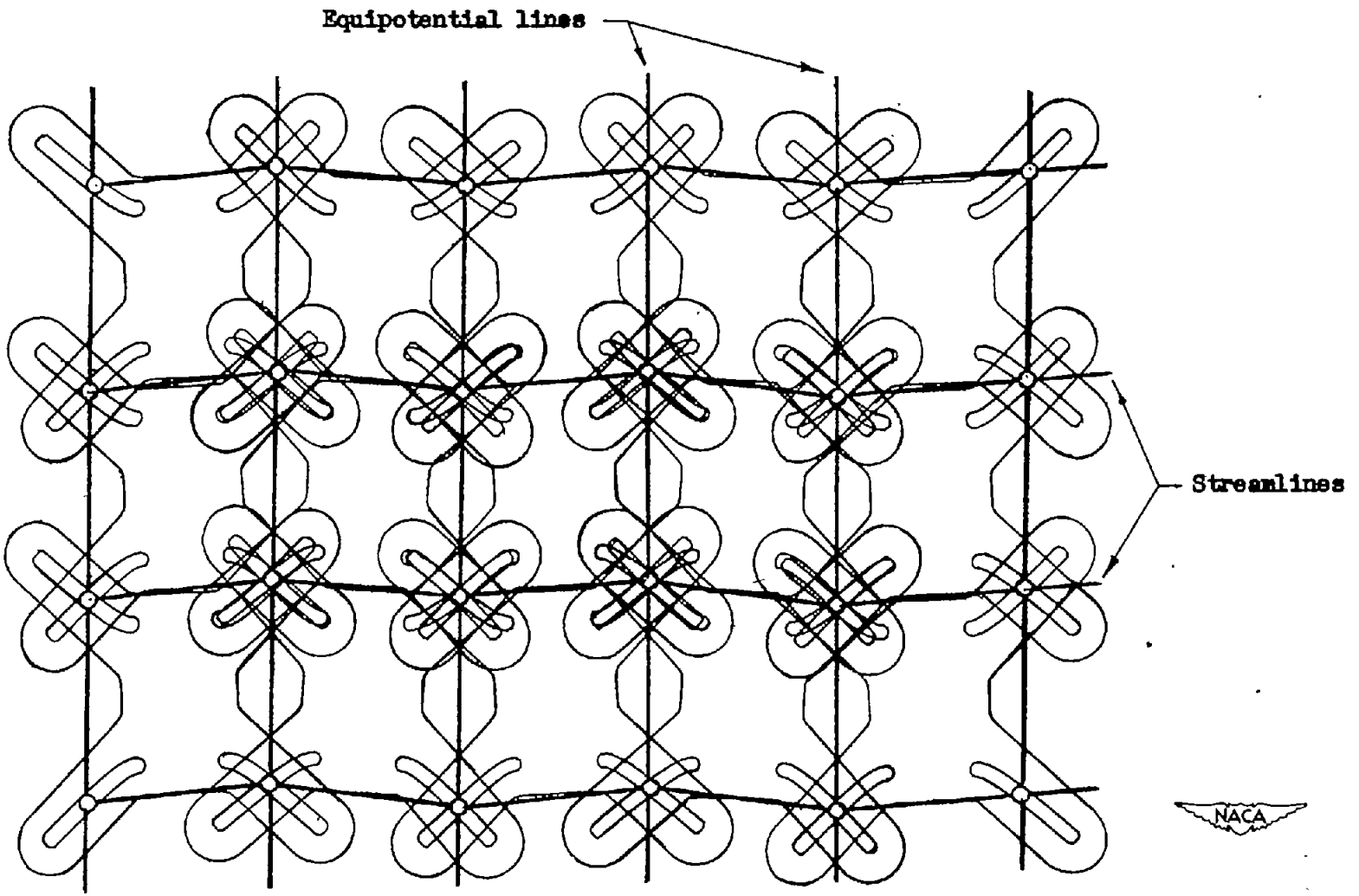

(b) Zigzag of streamlines.

Figure 4.- Concluded.

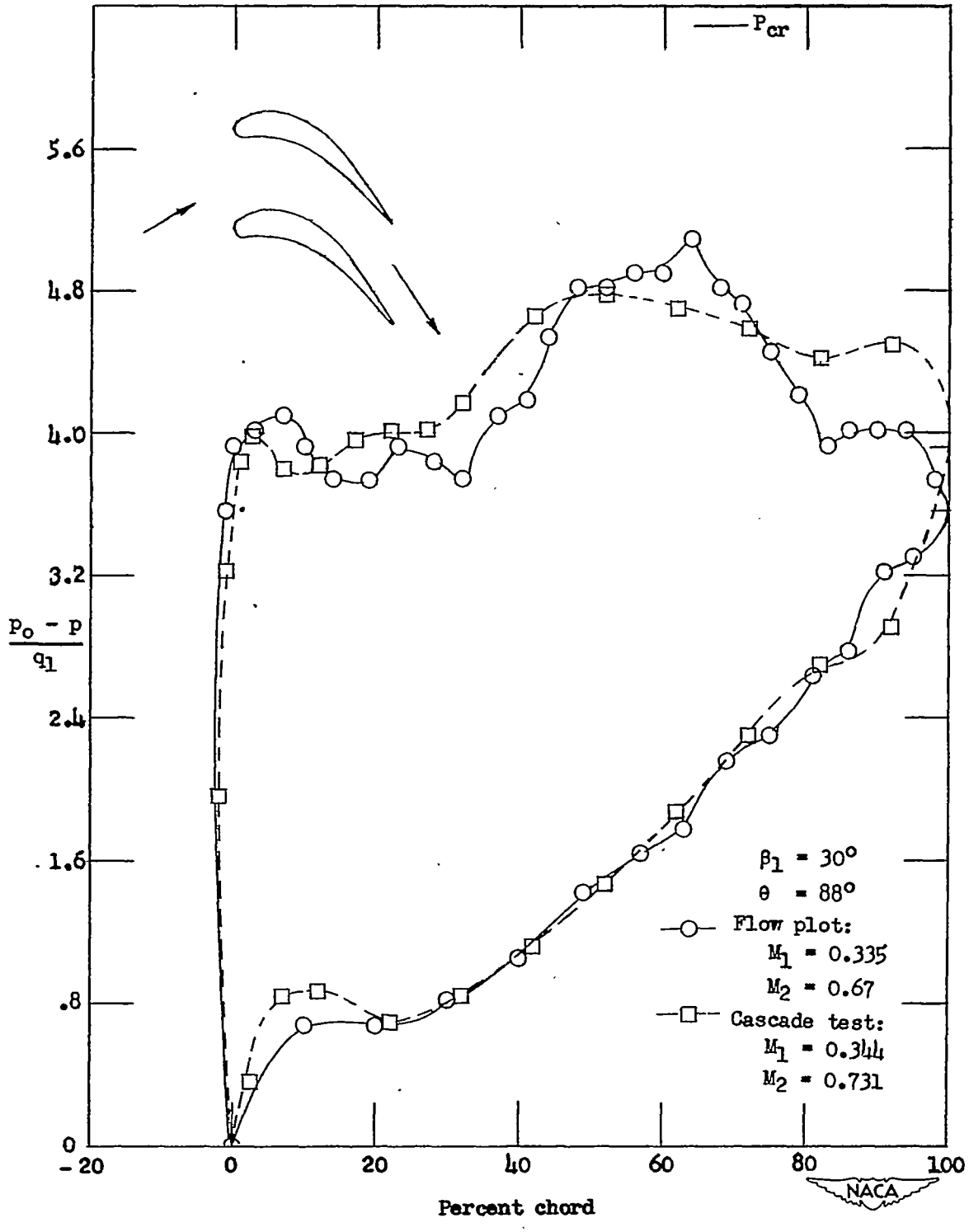

Figure 5.- Pressure distribution for turbine blade.

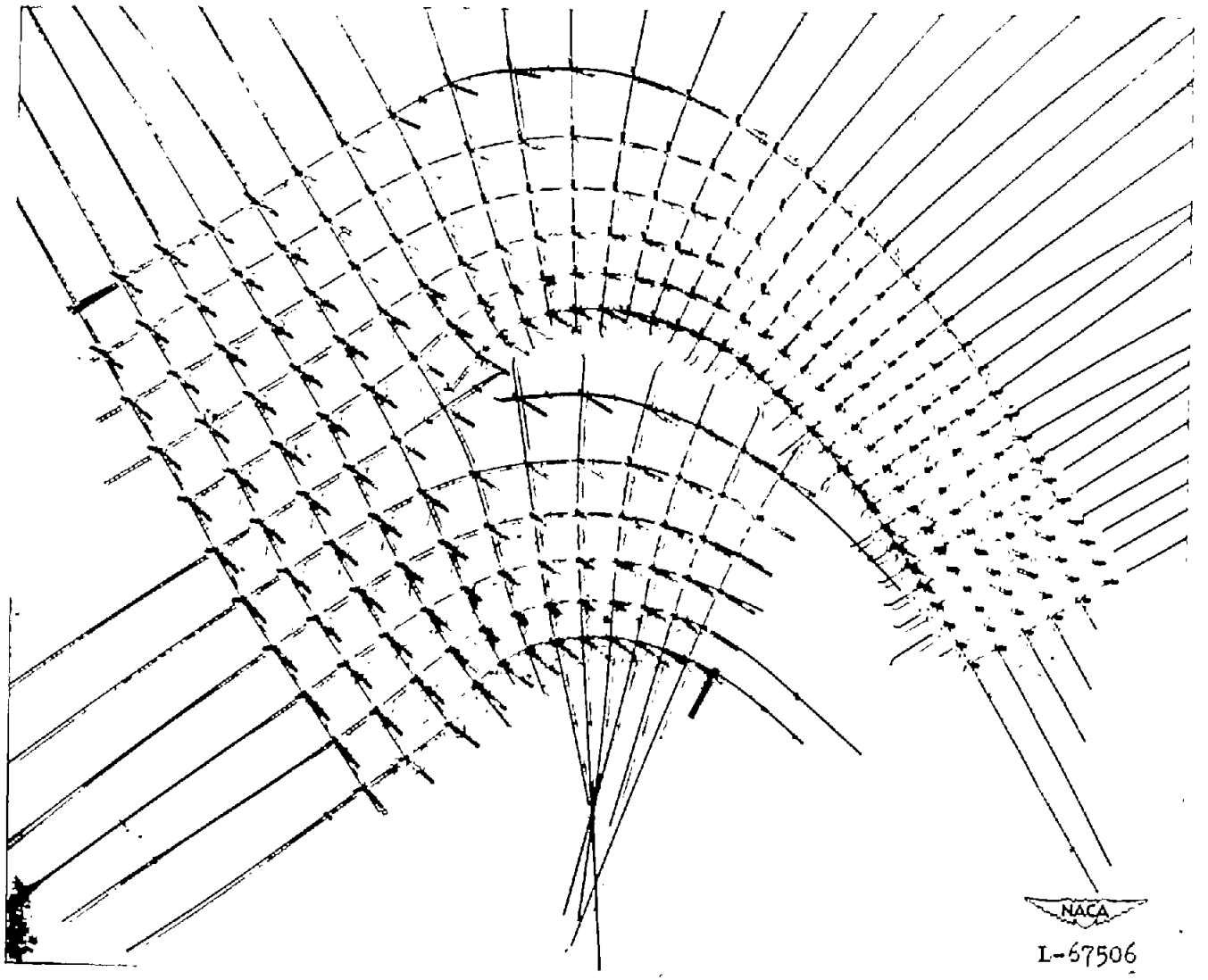

Figure 6.- Compressible-flow plot of turbine blade of figure 5.

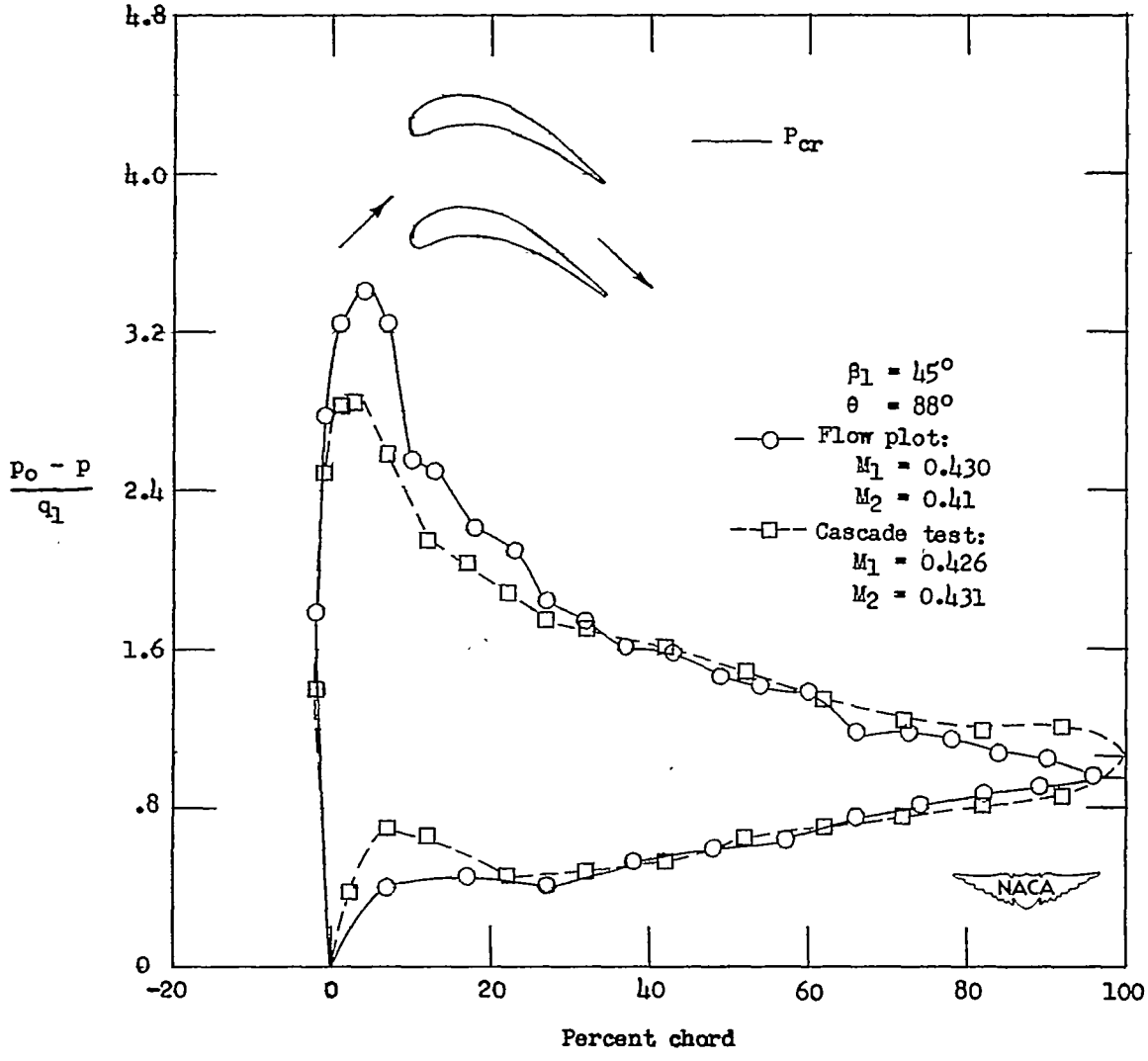

Figure 7.- Pressure distribution for turbine blade.

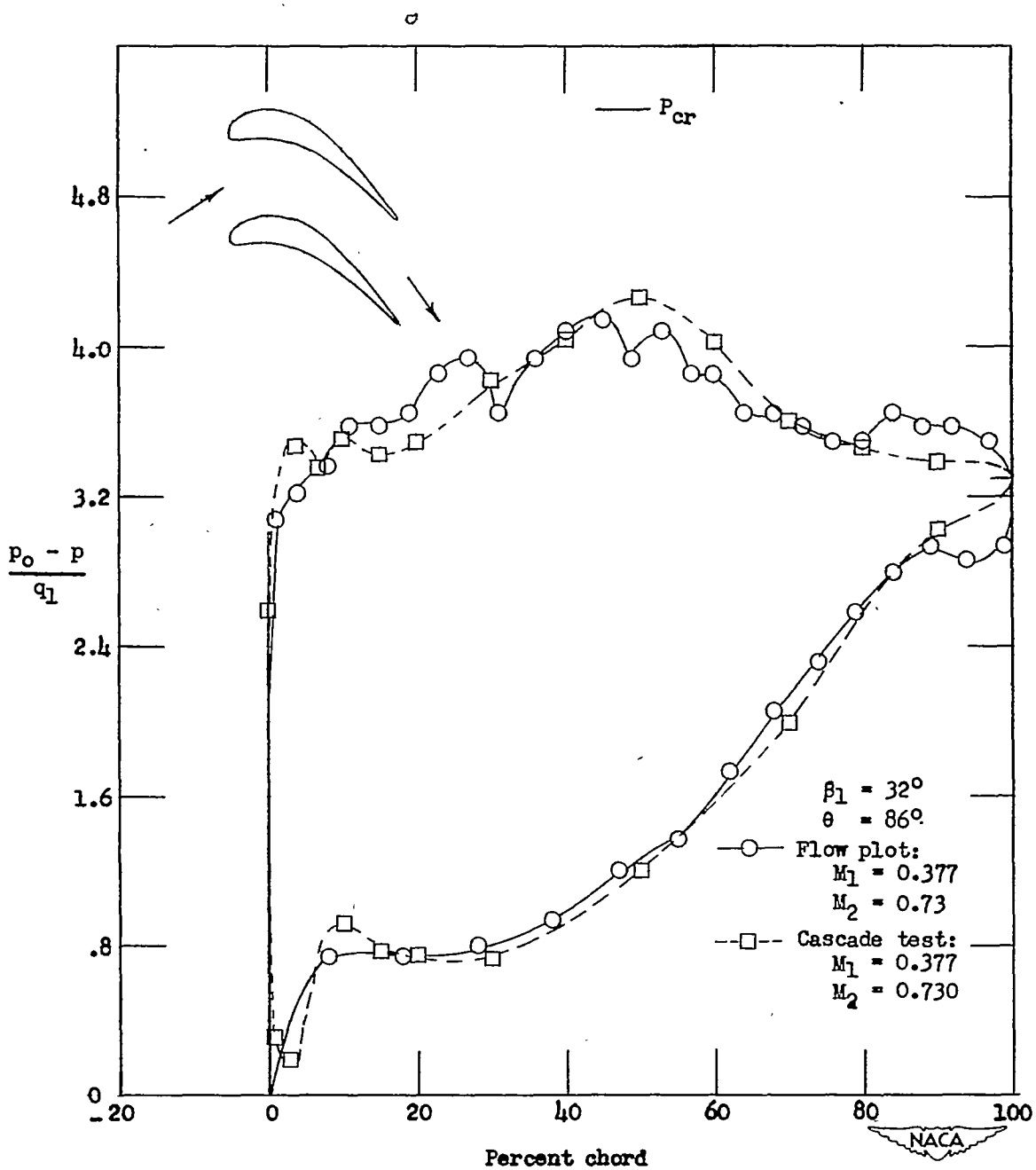

Figure 8.- Pressure distribution for turbine blade.

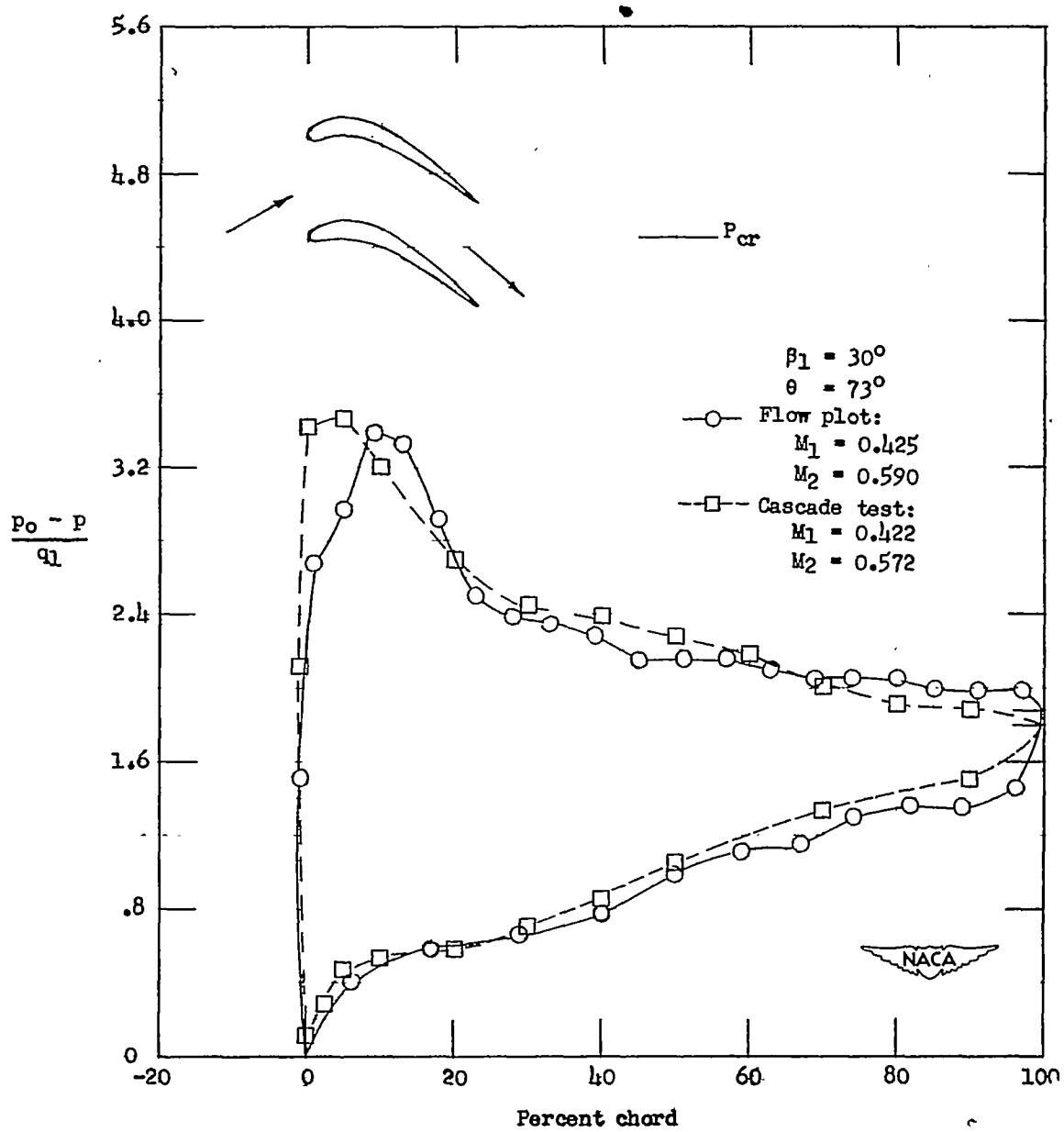

Figure 9.- Pressure distribution for turbine blade.

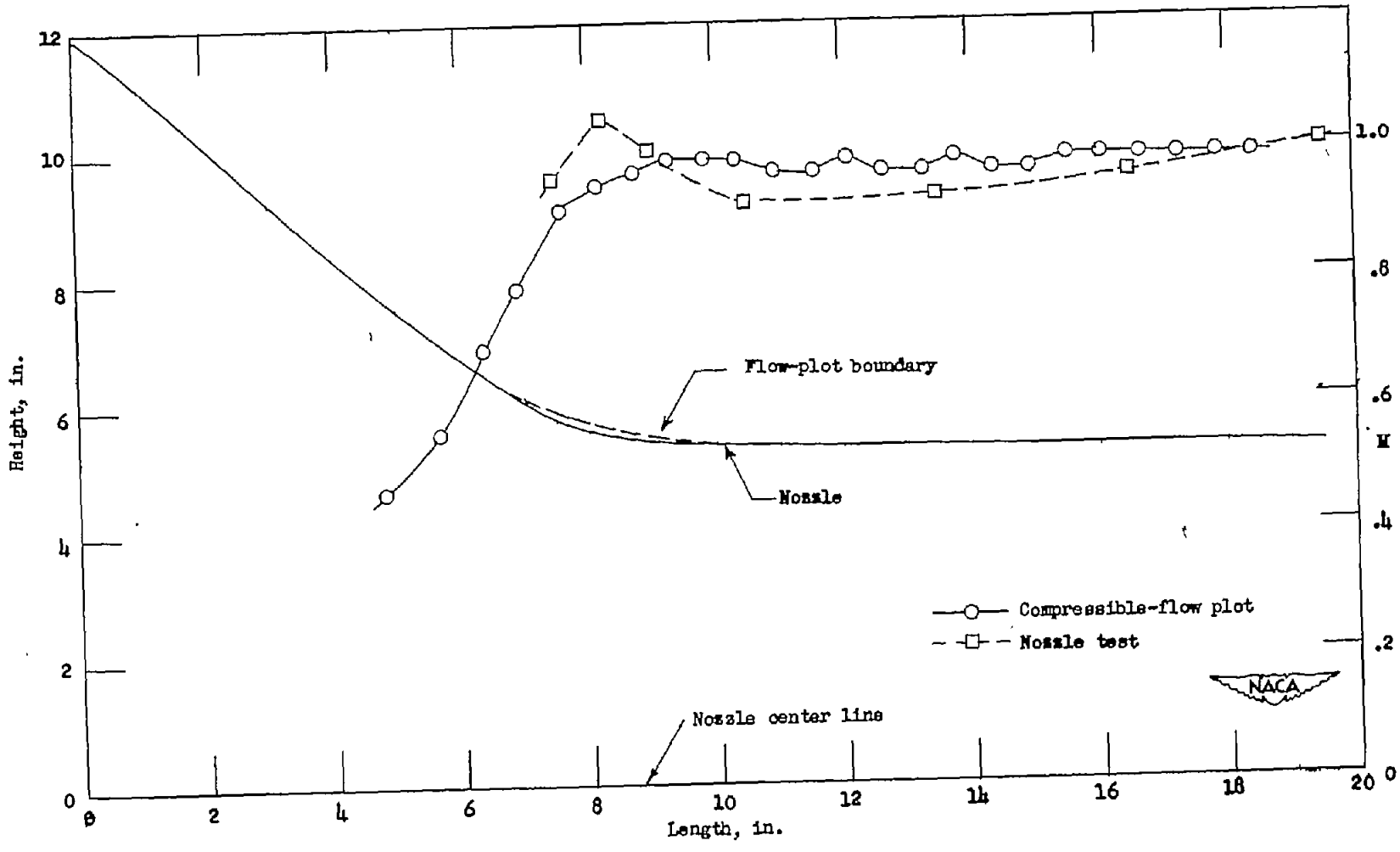

Figure 10.- Nozzle shape and Mach number distribution along nozzle surface in choked condition.

NACA-Langley - 4-1-48 - 1000